

Introduction

In vitro neuron morphology and viability analysis remains a key approach to evaluate the impact of chemical exposures on neuron health and function. Single-step live-cell dyes provide a robust and simplified solution for multiparametric image-based toxicity characterization. Automated benchtop imaging and analysis improves the scale, efficiency and reproducibility of in vitro neurotoxicity assays. In this proof-of-concept study, a panel of compounds representing a range of known toxicity phenotypes was evaluated on the Agilent BioTek imaging and analysis platform in a human iPSC-derived neuronal model. Automated image analysis quantitatively captured both neuro-specific and generalized toxicity signatures, corroborating multiple classes of previously reported effects. Follow up analysis using compartment-specific immunolabeling further resolved axon-specific neurotoxicity phenotypes. Together, these results validate the platform as a flexible, sensitive and robust solution for detecting diverse neurotoxic effects across a broad range of assay outcomes.

Experimental

Neuron reagents

Reagents were sourced from Sigma, unless noted. iPSC-derived neurons (FUJIFILM iCell GlutaNeurons, p/n R1061) were cultured according to product recommendations for media composition, culturing protocol, and plate coating procedure. Neurons were plated at 2,000 cells/well on 384-well microplates (Agilent, p/n 204628-100). At three hours post plating, a panel of fifteen treatments were added, resulting in a final concentration range of 0.001 to 10 μ M.

Neuron labeling

After 48 hours of drug treatment, live-cell dye calcein AM (Invitrogen, C34852), eTox Red (Agilent, p/n 711009), and Hoechst 33342 (p/n H3570) were added to a final concentration of 0.3, 0.3, and 0.6 μ M, respectively. Cells were incubated for ~1 hour at 37 $^{\circ}$ C before imaging began. Paraformaldehyde-fixed neuron cultures were labeled with antibodies detecting β -III-tubulin (Invitrogen), MAP2, and Hoechst 33342 nuclear counterstain.

Imaging

The Agilent BioTek Lionheart FX automated microscope automatically captured 20x magnification images for GFP, CY5, and DAPI widefield fluorescence channels in a 2 x 2 montage across each well. Laser autofocus was used for image capture focus. Similar performance should be expected when using other Agilent BioTek imaging instruments, including all Cytation cell imaging multimode readers that support multichannel live-cell fluorescence widefield imaging and laser autofocus.

Analysis

Image acquisition and analysis were performed with the Agilent BioTek Gen5 neurite outgrowth module. Dose-response visualization and analysis was also performed in Gen5 software. Additional statistical comparisons and plotting were performed in GraphPad Prism software.

Live-cell imaging and analysis platforms

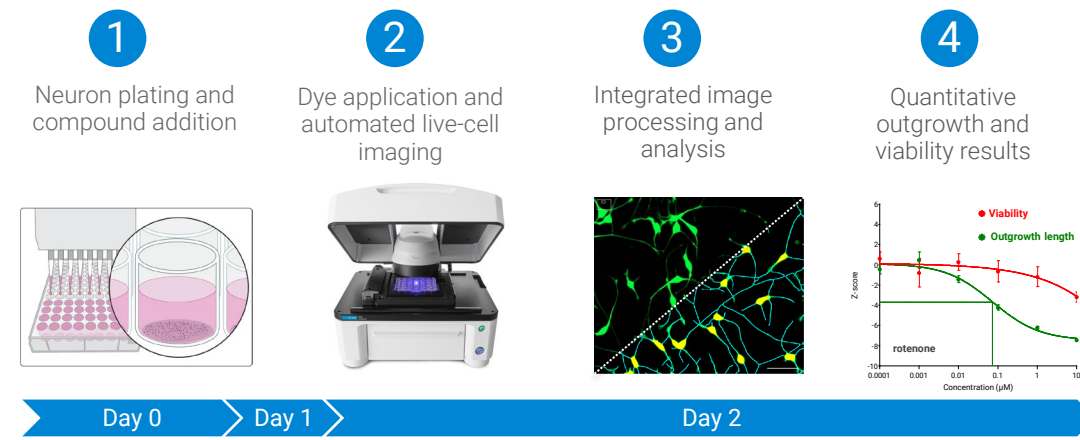


Figure 1. Agilent BioTek imaging systems compatible with live-cell neurotoxicity analysis.

Expanded materials and methods are available in the application note "Rapid, Image-Based Viability and Outgrowth Analysis for Neurotoxicity Assays."

Experimental

Assay overview



Validation of approach

Calcein AM: Single-dye viability and outgrowth analysis

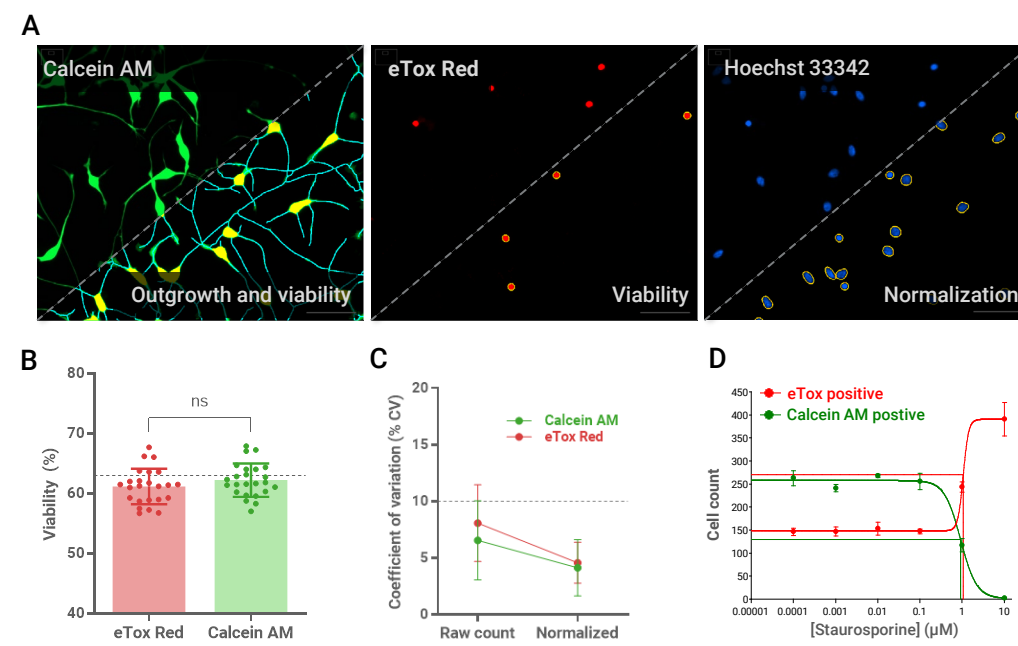


Figure 2. (A) Example images of calcein AM, eTox Red, and Hoechst 33342 live-cell staining of iPSC-derived neuron cultures. Calcein AM analysis identifies neurite outgrowth morphology and cell counts for viability. eTox Red labels non-viable cells as an orthogonal method for viability determinations. Hoechst 33342 labels all cells for normalization purposes. (B) Percent viable cell determinations for all control wells (n = 24) by eTox Red or calcein AM staining analysis. Individual well data are displayed over bars, showing mean and standard deviation. The dashed line corresponds to the initial cell viability measured at thaw. (C) Comparison of percent coefficient of variation (CV) of cell viability measurements before and after normalization with total cell counts from the Hoechst 33342 analysis. Data points indicate the mean and standard deviation of controls (N = 6 replicate sets, n = 4 wells each set). Raw cell counts across both methods demonstrate less than 10% CV (dashed line). Normalization further reduces %CV by ~3%. (D) Comparison of staurosporine treatment toxicity evaluated by eTox Red and calcein AM analysis. Data points correspond to the mean and standard deviation of replicate wells (n = 4) for each concentration, with a four-parameter fit overlay (solid lines) and corresponding EC₅₀/IC₅₀ interpolation (dashed lines).

Automated image analysis and z-score calculation

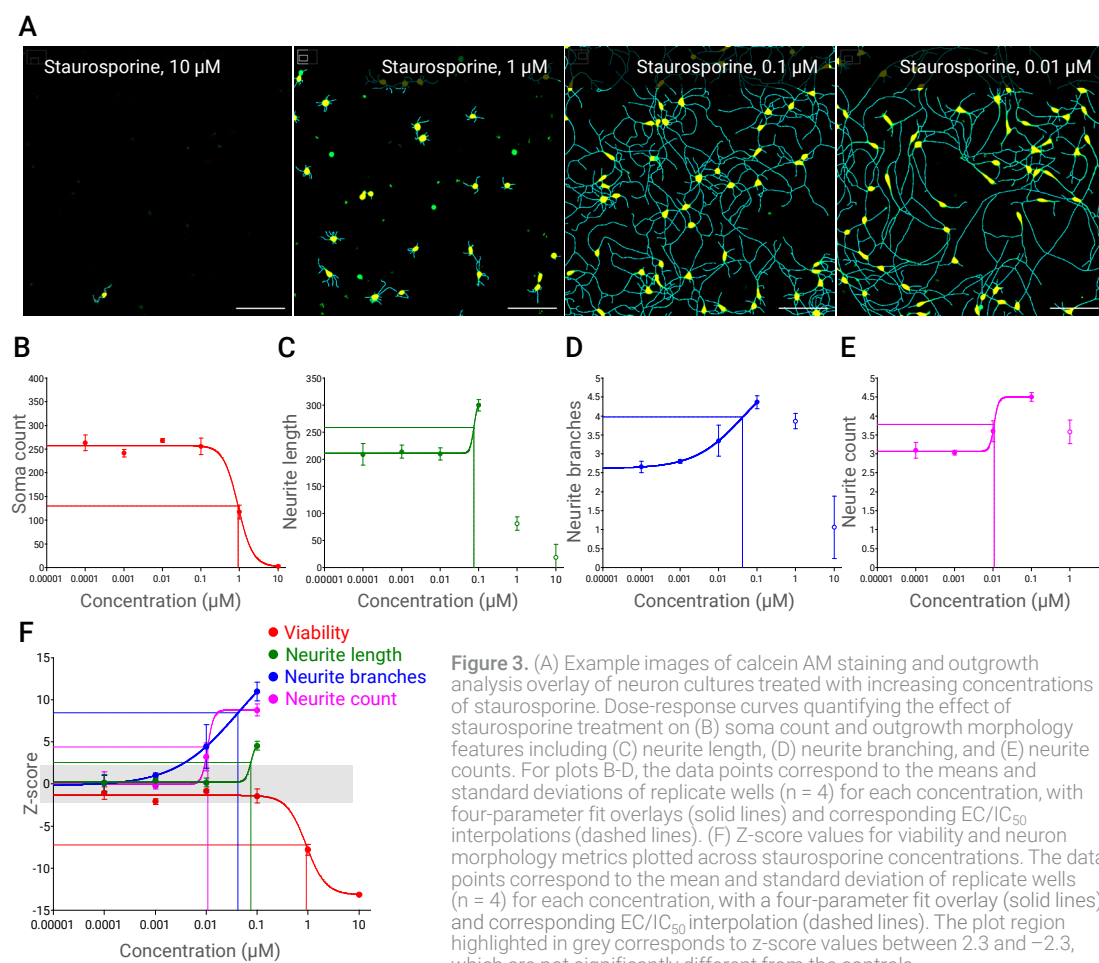


Figure 3. (A) Example images of calcein AM staining and outgrowth analysis overlay of neuron cultures treated with increasing concentrations of staurosporine. Dose-response curves quantifying the effect of staurosporine treatment on (B) soma count and outgrowth morphology features including (C) neurite length, (D) neurite branching, and (E) neurite counts. For plots B-D, the data points correspond to the means and standard deviations of replicate wells (n = 4) for each concentration, with four-parameter fit overlays (solid lines) and corresponding EC₅₀/IC₅₀ interpolations (dashed lines). (F) Z-score values for viability and neuron morphology metrics plotted across staurosporine concentrations. The data points correspond to the mean and standard deviation of replicate wells (n = 4) for each concentration, with a four-parameter fit overlay (solid lines) and corresponding EC₅₀/IC₅₀ interpolation (dashed lines). The plot region highlighted in grey corresponds to z-score values between 2.3 and -2.3, which are not significantly different from the controls.

Results and Discussion

Compound toxicity profile and MOA diversity

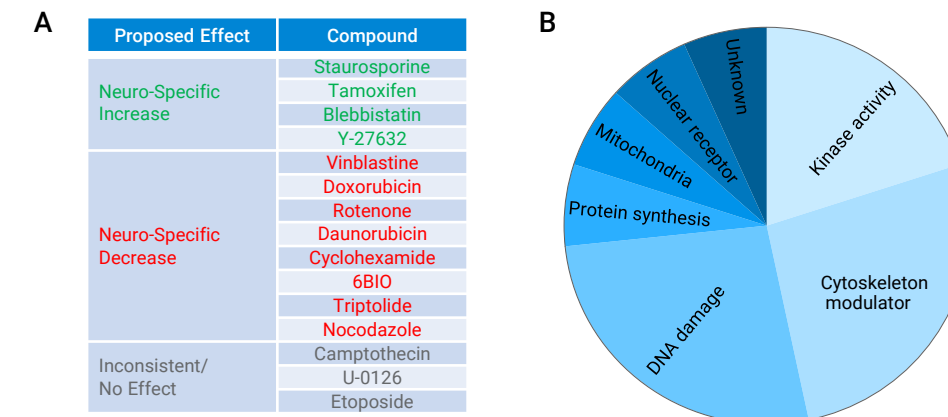


Figure 4. (A) List of potential neurotoxicants tested and their predicted effects based on previously published work across various neuronal model systems and techniques. (B) Summary of compound panel MOA class diversity.

Characterization of neurotoxic phenotypic profiles

Class 1: Reduced neurite length

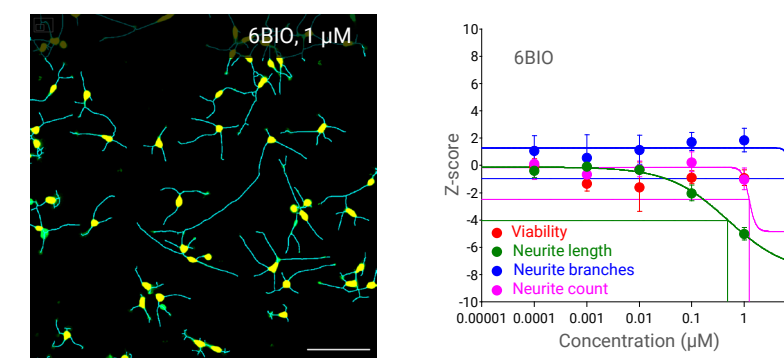


Figure 5. Dose-response profiles for neurotoxic treatments that generally reduced neurite outgrowth across morphology features. Example images and dose-response analysis for (A) 6BIO, (B) triptolide, and (C) cyclohexamide treatments, where concomitant decreases in both length and branching features of neuron morphology were observed. Six of the fifteen treatments demonstrated a similar effect profile, with or without significant viability effects observed in the concentration range tested. Data points correspond to the mean and standard deviation of replicate wells (n = 4) for each concentration, with a four-parameter fit overlay (solid lines) and corresponding EC₅₀/IC₅₀ interpolation (dashed lines).

Class 2: Increased neurite length

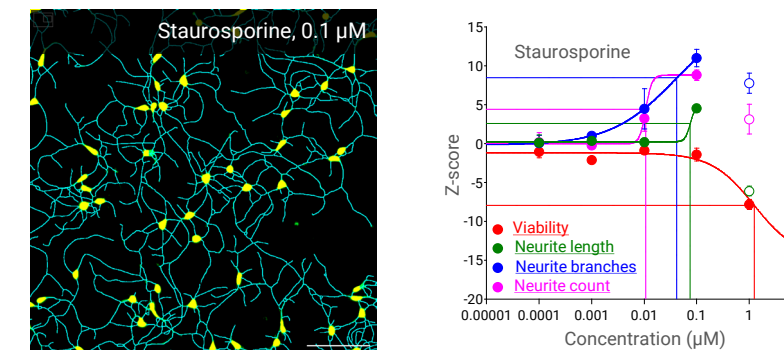


Figure 6. Dose-response profiles for neurotoxic treatments that generally increased neurite outgrowth across morphology features. Example images and dose-response analysis for (A) staurosporine and (B) tamoxifen treatments, where various outgrowth features were significantly enhanced; as shown. Three of the fifteen treatments demonstrated a similar effect profile, with or without significant viability effects observed in the concentration range tested. Data points correspond to the mean and standard deviation of replicate wells (n = 4) for each concentration, with a four-parameter fit overlay (solid lines) and corresponding EC₅₀/IC₅₀ interpolation (dashed lines).

Class 3: Reduced neurite length with increased branching

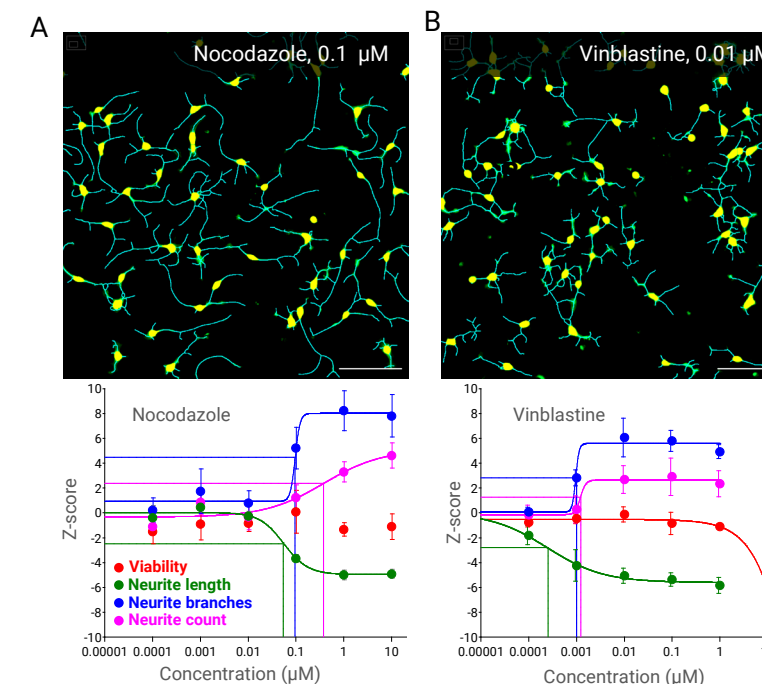


Figure 7. Dose-response profiles for neurotoxic treatments with varying effects on neurite outgrowth across morphology features. Example images and dose-response analysis for (A) nocodazole, and (B) vinblastine treatments, where decreases in neurite length and increases in neurite branching were observed. Two of the fifteen treatments demonstrated a similar effect profile, with or without significant viability effects observed in the concentration range tested. Both nocodazole and vinblastine share a common mechanism of action by inhibiting microtubule formation. Data points correspond to the mean and standard deviation of replicate wells (n = 4) for each concentration, with four-parameter fit overlay (solid lines) and corresponding EC₅₀/IC₅₀ interpolation (dashed lines).

Results and Discussion

Toxicity profile summary

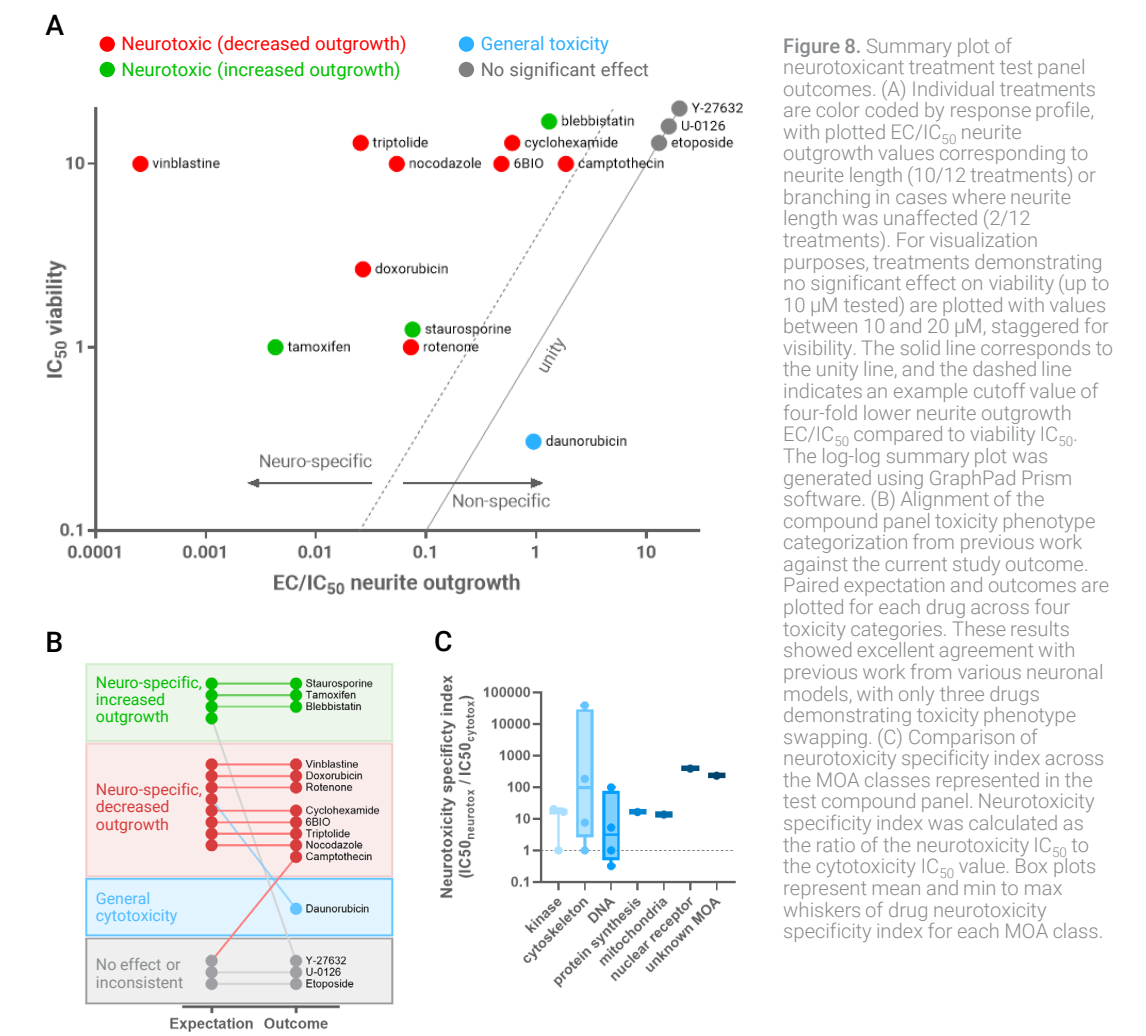


Figure 8. Summary plot of neurotoxicant treatment test panel outcomes. (A) Individual treatments are color coded by response profile, with plotted EC₅₀/IC₅₀ neurite outgrowth values corresponding to neurite length (10/12 treatments) or branching in cases where neurite length was unaffected (2/12 treatments). For visualization purposes, treatments demonstrating no significant effect on viability (up to 10 μ M tested) are plotted with values between 10 and 20 μ M, staggered for visibility. The solid line corresponds to the unity line, and the dashed line indicates an example cutoff value of four-fold lower neurite outgrowth EC₅₀ compared to viability IC₅₀. The log-log summary plot was generated using GraphPad Prism software. (B) Alignment of the compound panel toxicity phenotype categorization from previous work against the current study outcome. Paired expectation and outcomes are plotted for each drug across four toxicity categories. These results showed excellent agreement with previous work from various neuronal models, with only three drugs demonstrating toxicity phenotype swapping. (C) Comparison of neurotoxicity specificity index across the MOA classes represented in the test compound panel. Neurotoxicity specificity index was calculated as the ratio of the neurotoxicity IC₅₀ to the cytotoxicity IC₅₀ value. Box plots represent mean and min to max whiskers of drug neurotoxicity specificity index for each MOA class.

Immunolabeling identifies axon-specific neurotoxicity

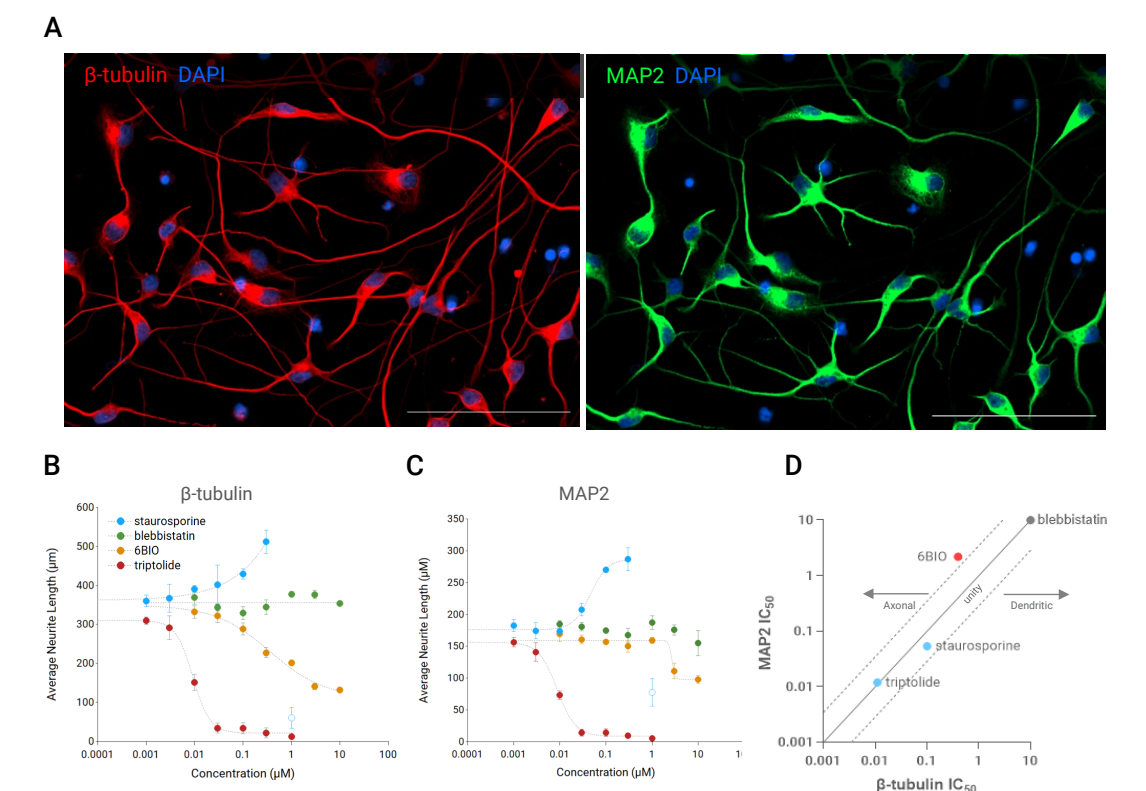


Figure 9. (A) Example images of iPSC-derived neurons fixed and stained with β -tubulin to evaluate total neurite length and MAP2 to measure dendritic length. (B) Dose-response plots of average neurite length measured for β -tubulin staining for four drugs. Data points indicate mean and standard deviation of replicates (n = 4). (C) Dose-response plots of average neurite length measured for MAP2 staining under the conditions from panel B. Data points indicate mean and standard deviation of replicates (n = 4). (D) Log-log plot comparing IC₅₀ values determined from β -tubulin and MAP2 staining. Only 6BIO showed significantly lower IC₅₀ values for β -tubulin than MAP2, suggesting specific reductions in axonal outgrowth.

Conclusions

- The Agilent BioTek automated microscopes and cell imaging multimode readers are a robust solution for neurotoxicity analysis
- Live-cell labeling with calcein AM dye captures essential viability and neurite outgrowth features, providing an effective alternative to antibody-based methods
- Agilent BioTek Gen5 software automated image analysis identifies salient neuron morphology features for dose-response analysis, providing a sensitive and efficient method to capture a broad range of neurotoxicity assay outcomes

For Research Use Only. Not for use in diagnostic procedures.
RA251029.545